The Differential Staurosporine-Mediated G_1 Arrest in Normal versus Tumor Cells Is Dependent on the Retinoblastoma Protein

Mollianne McGahren-Murray,[1] Nicholas H.A. Terry,[1] and Khandan Keyomarsi[1,2]

Departments of [1]Experimental Radiation Oncology and [2]Surgical Oncology, M.D. Anderson Cancer Center, Houston, Texas

Abstract

Previously, we reported that breast cancer cells with retinoblastoma (pRb) pathway–defective checkpoints can be specifically targeted with chemotherapeutic agents, following staurosporine-mediated reversible growth inhibition in normal cells. Here we set out to determine if the kinetics of staurosporine-mediated growth inhibition is specifically targeted to the G_1 phase of cells, and if such G_1 arrest requires the activity of wild-type pRb. Normal human mammary epithelial and immortalized cells with intact pRb treated with low concentrations of staurosporine arrested in the G_1 phase of the cell cycle, whereas pRb-defective cells showed no response. The duration of G_1 and transition from G_1 to S phase entry were modulated by staurosporine in Rb-intact cells. In pRb^+ cells, but not in Rb^- cells, low concentrations of staurosporine also resulted in a significant decrease in cyclin-dependent kinase 4 (CDK4) expression and activity. To directly assess the role of pRb in staurosporine-mediated G_1 arrest, we subjected wild-type ($Rb^{+/+}$) and $pRb^{-/-}$ mouse embryo fibroblasts (MEFs) to staurosporine treatments. Our results show that whereas $Rb^{+/+}$ MEFs were particularly sensitive to G_1 arrest mediated by staurosporine, $pRb^{-/-}$ cells were refractory to such treatment. Additionally, CDK4 expression was also inhibited in response to staurosporine only in $Rb^{+/+}$ MEFs. These results were recapitulated in breast cancer cells treated with siRNA to pRb to down-regulate the pRb expression. Collectively, our data suggest that treatment of cells with nanomolar concentrations of staurosporine resulted in down-regulation of CDK4, which ultimately leads to G_1 arrest in normal human mammary epithelial and immortalized cells with an intact pRb pathway, but not in pRb-null/defective cells. (Cancer Res 2006; 66(19): 9744-53)

Introduction

The majority of cancer patients treated today will receive either preoperative or postoperative chemotherapy. However, in many instances, chemotherapeutic regimens are limited by toxic side effects. Healthy proliferating cells, such as the epithelial lining of the intestine, hair follicle cells, and hematopoietic precursors, generally have fast doubling times (1, 2), making them very sensitive to the effects of chemotherapy.

Myelosuppression, in particular, results in dose reduction and incomplete administration of the prescribed regimens, allowing tumor cells to escape treatment and develop drug resistance (1–3). Therefore, agents and regimens are required that can exploit differential regulation between normal and tumor cells to protect normal cells from the toxic effects of chemotherapy.

One potential target that is differentially regulated between tumor and normal cells is the retinoblastoma (pRb) pathway, which is central to the G_1-S transition. Sequential phosphorylation of pRb by various cyclin/cyclin-dependent kinases (CDK) releases pRb from E2F, and enables E2F-dependent gene expression to initiate S and G_2-M phases of the cell cycle (4). The pRb protein, or its pathway components (p16, CDK4/6, and cyclin D1), is one of the most frequently altered pathways in many tumors (5–7). Such alterations in the pRb pathway lead to a deregulated cell cycle and the ability of the tumors to bypass the G_1 checkpoint (8, 9).

Our lab previously showed that differences in the G_1 checkpoint between normal and tumor cells can be used to protect normal cells while maintaining efficacy of chemotherapeutic agents against tumor cells. Using an *in vitro* model, we have described a two-step strategy that optimizes selective targeting of tumor cells (2). The first step involved using the protein kinase C (PKC) inhibitor staurosporine, which inhibits the proliferation of normal but not tumor cells in a reversible fashion. Subsequently, cells were treated with DNA-damaging agents (i.e., camptothecin or doxorubicin). By pretreating normal cells with staurosporine, the maximum tolerated dose of camptothecin was increased by 2 orders of magnitude. However, in tumor cells treated with staurosporine, the maximum tolerated dose remained unchanged. Of interest, we found that the protection observed was in a p53-independent and pRb-dependent manner. Other labs have similarly shown that the ability of staurosporine to mediate inhibition of cell proliferation is dependent on an intact pRb pathway (3, 10–13).

Staurosporine, a microbial alkaloid, was originally discovered as a general PKC inhibitor through screening of the bacterium *Streptomyces staurospores*. PKC represents a family of phospholipid-dependent serine/threonine kinase with multiple isoforms (α, βI, βII, δ, ε, γ, η, ι, μ, θ, and ξ) important for proliferation, differentiation, and malignant transformation. Targeting PKC has therefore the potential of modifying malignant growth (14). Staurosporine is a potent but nonselective inhibitor of PKC capable of inhibiting all the isoforms (15). Besides PKC, staurosporine has other targets as well, including CDK4/cyclin D1, CDK2/cyclin E, PKA, and mitogen-activated protein kinase (16, 17). The mechanism underlying the differential effects of staurosporine on the pRb pathway of normal and tumor cells remains unknown. Some have suggested that the effects of staurosporine on the cell cycle are mediated by a number of cell cycle regulators including cyclin E, cyclin D1, CDK2, p18, p21, and p27 (11, 12, 17–22). To further examine the mechanism for the differences in staurosporine action between normal and tumor cells, we developed an *in vitro* model consisting of cell lines with different pRb status. We used normal mortal and immortalized cells with an intact pRb pathway and compared them with immortalized or tumor cells with a defective pRb pathway. The two

Requests for reprints: Khandan Keyomarsi, Experimental Radiation Oncology, The University of Texas M.D. Anderson Cancer Center, 1515 Holcombe Boulevard, Box 66, Houston, TX 77030-4095. Phone: 713-792-4845; Fax: 713-794-5369; E-mail: kkeyomar@mdanderson.org.

doi:10.1158/0008-5472.CAN-06-1809

immortalized, nontumorigenic cell lines 76NE6 (pRb^+) and 76NE7 (pRb^-) are variants of the normal human mammary epithelial cell line 76N, which have been immortalized with the human papillomavirus 16E6 (degrades the p53 protein) or 16E7 (inactivates the pRb protein; refs. 23–30). We also directly assessed the role of pRb in staurosporine-mediated G_1 arrest in wild-type ($Rb^{+/+}$) and $pRb^{-/-}$ mouse embryo fibroblasts (MEFs) and Rb siRNA–treated breast cancer cells. Collectively, using the three different cell line models, our data suggest that the pRb pathway is the mediator of G_1 arrest following staurosporine treatment and that cells null/defective in the pRb pathway are refractory to the G_1-arresting abilities of staurosporine.

Materials and Methods

Cell lines, culture conditions, and materials. The 76NE6 and 76NE7 cell lines, a gift from Dr. V. Band (Northwestern University, Evenston, IL), were immortalized and cultured as previously described (30–32). The culture conditions for 76N and 81N normal cell lines, immortalized MCF-10A cell line, and breast cancer MDA-MB-231, HBL100, and MDA-MB436 breast cancer cell lines were previously described (33, 34). All cells were cultured and treated at 37°C in a humidified incubator containing 6.5% CO_2. Serum was purchased from HyClone Laboratories (Logan, UT) and cell culture medium was from Life Technologies, Inc. (Rockville, MD). Staurosporine was purchased from Roche Molecular Biochemicals (Indianapolis, IN). The materials for flow cytometry were from Sigma-Aldrich (St. Louis, MO) unless otherwise noted.

siRNA transfections. MDA-MB-231 cells (pRb^+) were transiently transfected with siRNA to pRb (Ambion, Austin, TX) per instructions of the manufacturer. Briefly, cells were harvested with 1× trypsin (Life Technologies) and inactivated with trypsin inhibitor (Sigma-Aldrich). The cell suspension was brought to a total volume of 1×10^5/mL in culture medium and kept warm in a 37°C in a humidified incubator. Serum- and growth factor–free medium that contained only 1% 1 mol/L HEPES was used for the transfection (ZAP medium). One hundred microliters of ZAP medium and 8 μL of siPORT Amine (Ambion) transfection reagent were incubated for 10 minutes at room temperature. Simultaneously, 100 μL of ZAP and 30 nmol/L of predesigned siRNA oligos to the *Rb1* gene (Ambion) were also incubated for 10 minutes at room temperature. The mixtures containing the transfection reagent and Rb siRNA oligos were then incubated together for an additional 10 minutes. Two hundred microliters of this mixture were then added to each well of an empty six-well plate. Cells (2.3×10^5; 2.3 mL) from the cell suspension were then added to each well and allowed to incubate for 24 hours, at which point cells were washed free of transfection reagents and fresh medium was added. Seventy-two hours after transfection, the cells were either treated with 4 nmol/L staurosporine or vehicle (DMSO) control. Cells were incubated for an additional 24 hours, harvested, and subjected to flow cytometric and Western blot analysis.

DNA content analysis. For determination of cell cycle distribution following staurosporine treatment, DNA content was measured by flow cytometry using staurosporine-treated cells that were harvested and stained with propidium iodide alone or in combination with 5-bromo-2-deoxyuridine (BrdUrd). Briefly, 24 hours after plating cells on 150-mm plates, the medium was removed and the cells were treated with staurosporine or fresh medium (control) for 48 hours. The cells were then harvested and 3×10^6 cells were washed with cold PBS. For propidium iodide staining, cell pellets were then fixed overnight with 70% ethanol. Cells were then washed in PBS and stained with a solution of 10 μg/mL propidium iodide and 20 μg/mL RNase A in PBTB (PBS with 0.5% Tween 20 and 0.5% bovine serum albumin). Twenty-four hours after staining, 1×10^6 cells were filtered and allowed to incubate at 37° for at least 30 minutes. Cell cycle distribution was acquired with a FACScalibur (Becton Dickinson, San Jose, CA) and the percentage of cells in each phase of the cell cycle was analyzed with ModFit software.

For the pulse-chase BrdUrd labeling experiments, the cells were labeled for 20 minutes with 1 μmol/L BrdUrd at 37°C, followed by either a fresh medium wash or medium plus 4 nmol/L of staurosporine. Time points were set every 3 hours, and after harvesting, the cells were then fixed overnight with 60% ethanol and processed for BrdUrd staining as previously described (35). For the determination of the fraction of labeled divided cells (f_{ld}), the number of divided and undivided labeled (i.e., BrdUrd positive) cells were calculated and divided by the total number of cells stained with propidium iodide.

For the synchronization experiments with nocodazole, cells were treated with either nocodazole alone, staurosporine alone, or nocodazole plus staurosporine. In both cases in which the cells were treated with nocodazole, the cells were treated with 0.125 μg/mL nocodozole for 12 hours and then washed with either fresh medium (nocodazole alone) or medium plus 4 nmol/L staurosporine (nocodazole plus staurosporine). Cells were harvested every 3 hours and subjected to fluorescence-activated cell sorting analysis.

Western blot analysis and immunoprecipitation kinase assays. Cell lysates were prepared and subjected to Western blot analysis as previously described (36). Following harvesting, the cells were resuspended in protease phosphatase buffer (25 μg/mL leupeptin, 25 μg/mL aprotinin, 10 μg/mL pepstatin, 1 mmol/L benzamidine, 10 μg/mL soybean trypsin inhibitor, 0.5 mmol/L phenylmethylsulfonyl fluoride, 50 mmol/L NaF, 0.5 mmol/L sodium orthovanadate) in solution A (27 mmol/L HEPES, 10 mmol/L glucose, 3.3 mmol/L KCl, 13 mmol/L NaCl, 0.5 mmol/L Na_2HPO_4, pH 7.6) to prevent protein degradation. Cell lysates were homogenized by sonication followed by centrifugation at 100,000 × *g*. The soluble supernatant fraction was removed and protein concentrations were determined with the Bradford assay (Bio-Rad, Hercules, CA). For Western blot analysis, 50 μg of protein lysate from each condition were electrophoresed in each lane of a 10% (CDK4, CDK2, and actin), 13% (p21, p27 and actin), or 7% (pRb and actin) SDS-PAGE gel and transferred to polyvinylidene difluoride membrane (NEN Life Sciences Products, Inc., Boston, MA) at 4°C, either overnight at constant voltage of 35 mV or for 2.5 hours at a constant voltage of 85 mV. The blots were blocked overnight in BLOTTO (5% nonfat dry milk in 20 mmol/L Tris, 137 mmol/L NaCl, 0.25% Tween, pH 7.6). After washing in TBST (20 mmol/L Tris, 137 mmol/L NaCl, 0.05% Tween, pH 7.6), the blots were incubated in primary antibody for 2.5 hours. Primary antibodies used were pRb (Santa Cruz Biochemicals, Santa Cruz, CA), p21 (Oncogene Research Products/Calbiochem, San Diego, CA), p27, CDK4, and CDK2 (Transduction Laboratories, Lexington, KY), all at 1 μg/mL, and actin (Chemicon, Temecula, CA) at 0.1 μg/mL. After incubation with primary antibody, the blots were washed and then incubated in BLOTTO with a secondary antibody and horseradish peroxidase conjugate (Pierce Biotechnology, Inc., Rockford, IL) at a dilution of 1:5,000 for 1 hour. Finally, the blots were again washed and developed in chemiluminescence reagent (NEN/Perkin-Elmer Life Sciences Products, Boston, MA) as directed by the manufacturer.

For CDK4 kinase assay, cell extracts (250 μg) were immunoprecipitated with 5 μL of monoclonal antibody to CDK4 (BD Transduction Laboratories, San Jose, CA) in lysis buffer [50 mmol/L Tris-HCl (pH 7.5), 200 mmol/L NaCl, 0.5% NP40, and 1 mmol/L DTT]. The protein/antibody mixture was incubated with protein G-sepharose beads (Amersham Biosciences AB, Uppsla Sweden) overnight and then washed four times with lysis buffer and four times with kinase buffer [20 mmol/L Tris-HCl (pH 7.5), 10 mmol/L $MgCl_2$, 1 mmol/L DTT, and 1 mmol/L EGTA]. The immunoprecipitates were then incubated with kinase buffer containing 60 μmol/L cold ATP, 5 μCi of [γ-^{32}P]dATP, and 1 μg of glutathione *S*-transferase (GST)-Rb (Rb-769; Santa Cruz Biochemicals) in a final volume of 20 μL at 37°C for 30 minutes. Adding an equal amount of loading dye to the mix stopped the reaction and the samples were then boiled and resolved on a 10% SDS-PAGE gel. The gels were stained, destained, dried, and exposed to X-ray film. For quantitation of relative kinase activity, the bands corresponding to GST-Rb were analyzed on a phosphoimager Typhoon 9400 machine (Amersham Biosciences).

Results

The G_1 phase of the cell cycle is enriched in staurosporine-treated pRb^+, but not pRb^-, cells. To assess if the pRb status of cells could be a determinant of their sensitivity to staurosporine,

we used a panel of retinoblastoma positive (pRb$^+$) and retinoblastoma negative (pRb$^-$) cell lines and treated them with staurosporine over a 48-hour time period. The pRb$^+$ cell lines examined included two normal mortal human mammary epithelial cell lines (81N and 76N), which were derived from reduction mammoplasty specimens (32), and an immortalized, nontumorigenic cell line, 76NE6. The pRb$^-$ cells consisted of a tumorigenic breast cancer cell line, MDA-MB436, a nontumorigenic SV40 transformed cell line, HBL100, and an immortalized, nontumorigenic cell line 76NE7. The 76NE6 (pRb$^+$) and 76NE7 (pRb$^-$) cell lines are variants of the normal human mammary epithelial cell line 76N, which have been immortalized with the human papillomavirus 16E6 (degrades the p53 protein) or 16E7 (inactivates the pRb protein; refs. 23–30). The cells were then harvested and processed for flow cytometric analysis with propidium iodide to stain the cells for DNA content (Fig. 1). The DNA histogram data of 76NE6 and 76NE7 cells treated with 0 or 4 nmol/L staurosporine reveals that following treatment, 76NE6 cells accumulated in G_1 with a concomitant reduction in S phase, whereas 76NE7 showed no significant perturbation in cell cycle phase distribution (Fig. 1*A*). Similarly, all the pRb$^+$ cell lines (81N, 76N, and 76NE6) examined responded to staurosporine by accumulation of cells in G_1 phase (Fig. 1*B*), whereas all the pRb$^-$ cell lines (76NE7, MDA-MB436, and HBL100) showed little to no perturbation in the G_1 phase of the cell cycle in response to

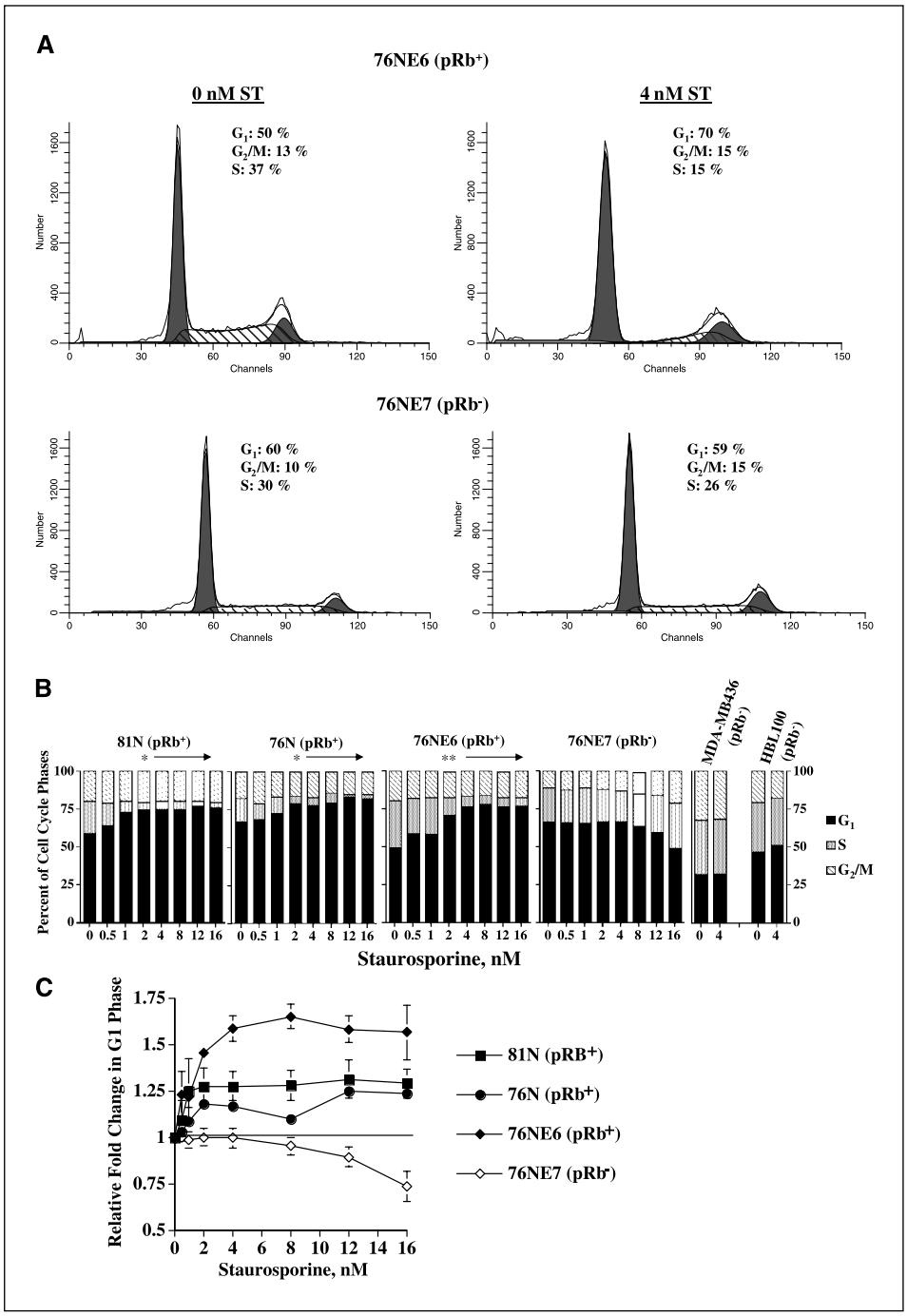

Figure 1. Staurosporine enriches cells in the G_1 phase of the cell cycle in pRb$^+$ but not in pRb$^-$ cells. *A,* pRb$^+$ (76NE6) and pRb$^-$ (76NE7) cells were treated with either a control amount of DMSO or 4 nmol/L staurosporine (*ST*). Cells were harvested after 48 hours and cell cycle distribution was measured by flow cytometry. *A,* raw histogram data for each cell line; *top,* pRb$^+$ cells; *bottom,* pRb$^-$ cells. *B,* cell cycle distribution in six different breast epithelial cell lines treated with staurosporine. Normal cell strains (81N and 76N) p53 and pRb inactivated variants of 76N (76NE6 and 76NE7) were treated with seven concentrations of staurosporine (0.5-16 nmol/L) and pRb-null/mutant breast cancer cell lines (MDA-MB436 and HBL100) were treated with one concentration of staurosporine (4 nmol/L) for 48 hours. Cell cycle distribution was measured by flow cytometry and the percent of each cell cycle phase is shown in a bar graph form with the G_1 (*solid black columns*), S (*gray columns*), and G_2-M (*hatched columns*) phases for each of the cell lines. Statistical calculations were done with GraphPad Prism 4 for Macintosh. The paired *t* test was done with a 95% confidence interval: *, $P = 0.05$; **, $P = 0.001$. *C,* relative fold change calculated from the full seven concentrations of staurosporine for the three pRb$^+$ cell lines (81N, 76N, and 76NE6) and the pRb$^-$ cell line (76NE7). The relative fold change was calculated by dividing the staurosporine-treated cells in G_1 phase by the control cells (0 nmol/L staurosporine) in G_1 phase.

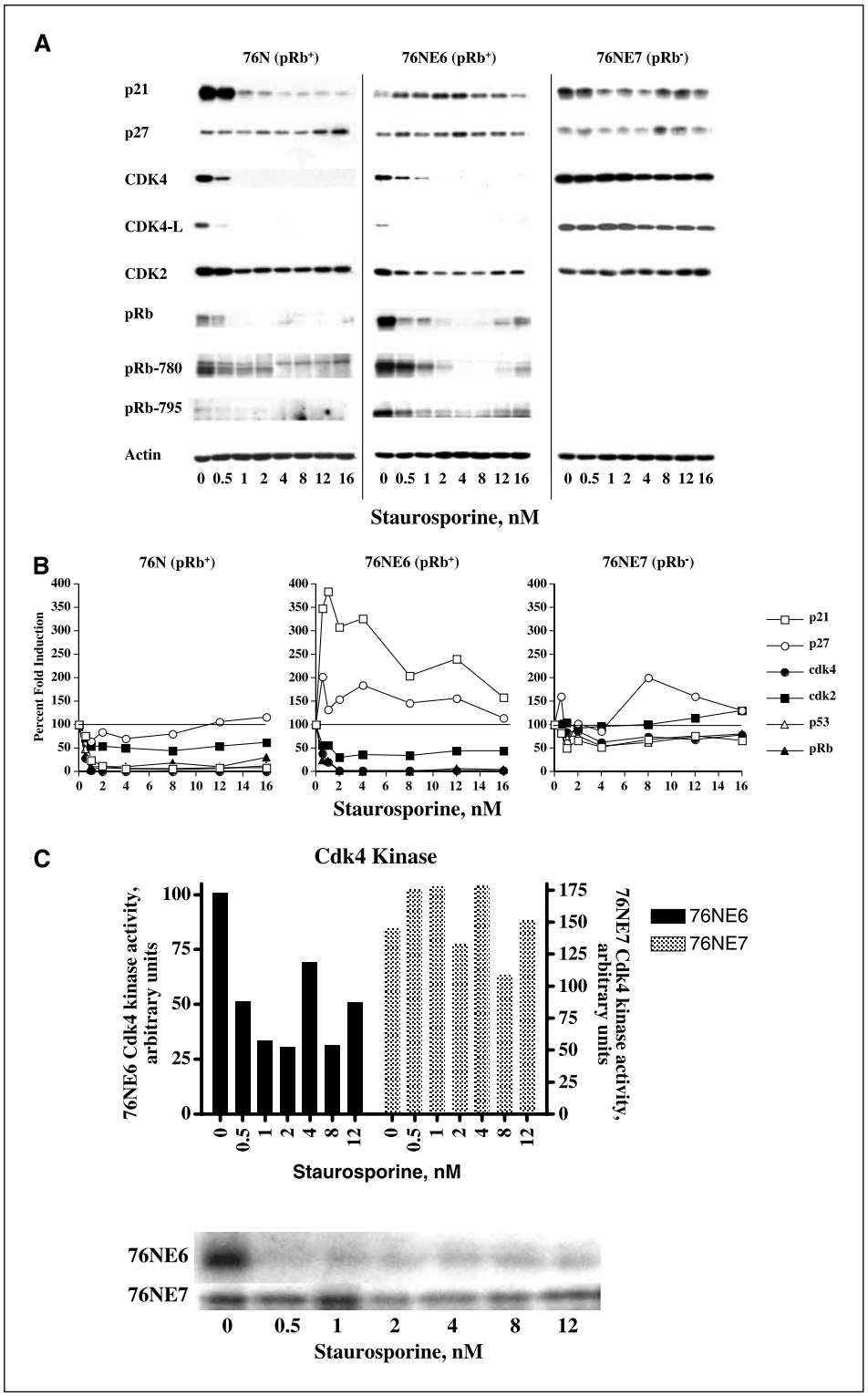

Figure 2. Staurosporine has a differential effect on cell cycle proteins in Rb^+ versus pRb^- cells. *A,* 76N human mammary epithelial cells and immortalized variants of 76N (76NE6 and 76NE7) were treated with the indicated concentrations of staurosporine for 48 hours. Following treatment, cell lysates were prepared and subjected to Western blot analysis with the indicated antibodies and actin for equal loading. *B,* densitometry data for each individual lane and antibody were calculated and compared with that of an actin control for that lane. Fold change is calculated by comparing the lanes treated with staurosporine to the 0 nmol/L control. *C,* for CDK4 GST-Rb kinase activity, equal amounts of protein (250 μg) from cell lysates were prepared from each cell line and immunoprecipitated with anti-CDK4 antibody (BD Transduction Laboratories) and protein G-sepharose beads (Amersham Biosciences) using GST-Rb (Rb-769; Santa Cruz Biochemicals) as a substrate. For each cell line, we show the resulting autoradiogram of the histone H1 SDS-PAGE and the quantitation of the GST-Rb associated kinase activities following phosphoimaging. The numbers on the left ordinate for the bar graph refer to counts per minute obtained from GST-Rb kinase assay for the 76NE6 cell line and the right ordinate numbers refer to the 76NE7 cell line.

staurosporine over the concentration ranges examined (Fig. 1*B* and *C*). Specifically, pRb^+ cells accumulated in G_1 (from 50% to 70% of cells) with a concomitant decrease in the S phase and little or no change in the G_2-M phase of the cell cycle. In 76NE7 cells, we observed a 12% decrease in the number of cells in the G_1 phase of the cell cycle at the highest concentrations of staurosporine (16 nmol/L) examined, with a concomitant increase in both the S and G_2-M phases of the cell cycle. These results suggest that the pRb protein is an important mediator in the response of cells to staurosporine treatment.

Staurosporine down-regulates pRb and CDK4 levels and activities in pRb^+ cells. Because the staurosporine-mediated G_1 enrichment was observed in the pRb^+ cells, but not in the pRb^- cells, we next sought to determine the expression of what proteins,

if any, are modulated differentially in the pRb^+ cells versus pRb^- cells in response to staurosporine. To this end, the pRb^+ (76N and 76NE6) and pRb^- (76NE7) cells were treated for 48 hours with a range of concentrations of staurosporine and were examined for the expression of key cell cycle proteins. These analysis showed that the levels of CDK4 and pRb and the phosphorylation status of pRb were significantly down-regulated in response to staurosporine in the pRb-positive 76N and 76NE6 cells, but not in 76NE7 cells (Fig. 2*A* and *B*). Specifically, densitometric analysis showed that treatment of pRb^+ cells with only 0.5 nmol/L staurosporine results in a 3- and 4-fold decrease in protein levels of CDK4 in the 76N and 76NE6 pRb^+ cells, respectively (Fig. 2*B*). In the pRb^- 76NE7 cells, CDK4 levels were minimally modulated by staurosporine. Similar to CDK4, pRb total levels and its CDK4-specific phosphorylation were down-regulated in both 76N and 76NE6 cells. The CDK inhibitor protein p21 is also down-regulated in response to staurosporine in 76N cells. This decrease, however, occurs in a p53-dependent fashion as the levels of p21 are also down-regulated in 76NE7 but not in 76NE6 cells. The levels of p27 and CDK2 were minimally modulated in all the three cell lines.

To examine if the down-regulation of CDK4 by staurosporine in 76NE6 results in the inhibition of CDK4 activity in these cells, we measured CDK4 kinase activity using GST-Rb as a substrate in both 76NE6 and 76NE7 cells treated with staurosporine. The results show that, in response to staurosporine, the CDK4 kinase activity is decreased in 76NE6 cells, whereas the kinase activity remains unabated in 76NE7 cells (Fig. 2*C*). These results suggest that the decrease in CDK4 kinase activity could account for staurosporine-mediated G_1 arrest in 76NE6 cells.

Lack of G_1 arrest of normal pRb^+ cells by PKC inhibitor K252A. Because staurosporine was originally discovered as a general PKC inhibitor, we next set out to determine if inhibition of PKC could also result in G_1 arrest of cells. To this end, we treated 76NE6 cells with increasing concentrations of a pure PKC inhibitor (K252A) for 48 hours. Flow cytometric analysis revealed that K252A had very little effect on the cell cycle of 76NE6, resulting in no change in G_1, S, or G_2 DNA content at low concentrations of the drug. K252A did not increase the G_1 phase at any concentration examined. The only cell cycle perturbation detected was accumulation of cells in G_2-M phase following treatment of cells with high concentrations of K252A (>65 nmol/L). (Similar G_2-M accumulation was observed when 76NE6 and 76NE7 cells were treated with concentrations of staurosporine >32 nmol/L; data not shown.) Western blot analysis of K252A-treated cells revealed a different pattern of expression of key cell cycle proteins compared with the staurosporine-treated cells (Fig. 3*C*). For example, in response to K252A, the levels of p21, p27, CDK4, and pRb all increased at the highest concentrations, the opposite of what was observed with staurosporine treatment (Fig. 2). Because K252A did not mediate G_1 arrest or modulate the levels of key cell cycle proteins at concentrations that inhibit PKC, the G_1 arrest mediated by staurosporine is most likely independent of PKC inhibition.

Staurosporine inhibits S-phase synthesis and progression in pRb^+ cells, but not in pRb^- cells. The results from the DNA histogram analysis (Fig. 1) suggested that staurosporine mediates G_1 arrest concomitant with a decrease of cells in S phase. However, such analysis is not sufficient to examine the rate and progression of DNA synthesis in response to staurosporine treatment. To directly address this question, we used a three-pronged approach to measure the rate of DNA synthesis and progression of S-phase BrdUrd incorporation into DNA. Initially, we examined the temporal effect of staurosporine on the cascade of events leading to G_1 arrest of cells. For this purpose, the staurosporine-responsive pRb^+ 76NE6 cells were treated with 4 nmol/L staurosporine and harvested for flow cytometry and BrdUrd analysis at 3-hour intervals for 24 hours to examine DNA content and modulation of rate of DNA synthesis (Fig. 4). Flow cytometry reveals that G_1 arrest initiates as early as 3 hours after treatment (Fig. 4*A*). This is further confirmed by a decrease in the BrdUrd staining, indicating a decrease in the rate of DNA synthesis (Fig. 4*B*). To determine whether the effect of staurosporine was reversible, following 24 hours of continuous exposures of cells to 4 nmol/L staurosporine,

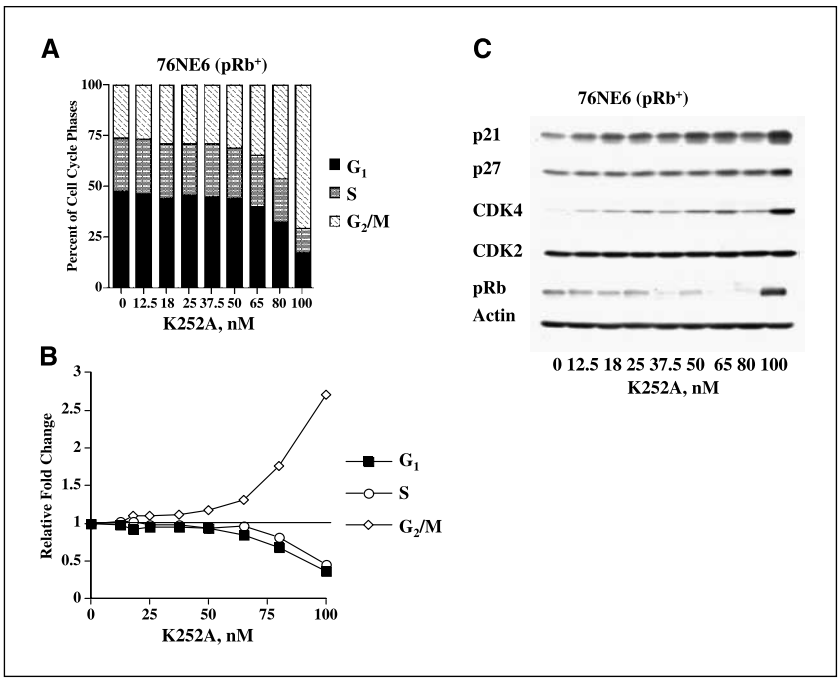

Figure 3. Inhibition of PKC does not mediate G_1 arrest. *A,* pRb^+ 76NE6 cells were treated with the indicated concentrations of K252A, a specific PKC inhibitor, and samples were subjected to flow cytometry and the percent of each cell cycle phase is shown in a bar graph form with the G_1 (*solid black columns*), S (*gray columns*), and G_2-M (*hatched columns*) phases for each cell line. *B,* relative fold change is calculated by dividing all of the staurosporine-treated cells in G_1 phase by the control cells (0 nmol/L staurosporine) in G_1 phase. *C,* following treatment with K252A, cell lysates were prepared and subjected to Western blot analysis with the indicated antibodies and actin for equal loading.

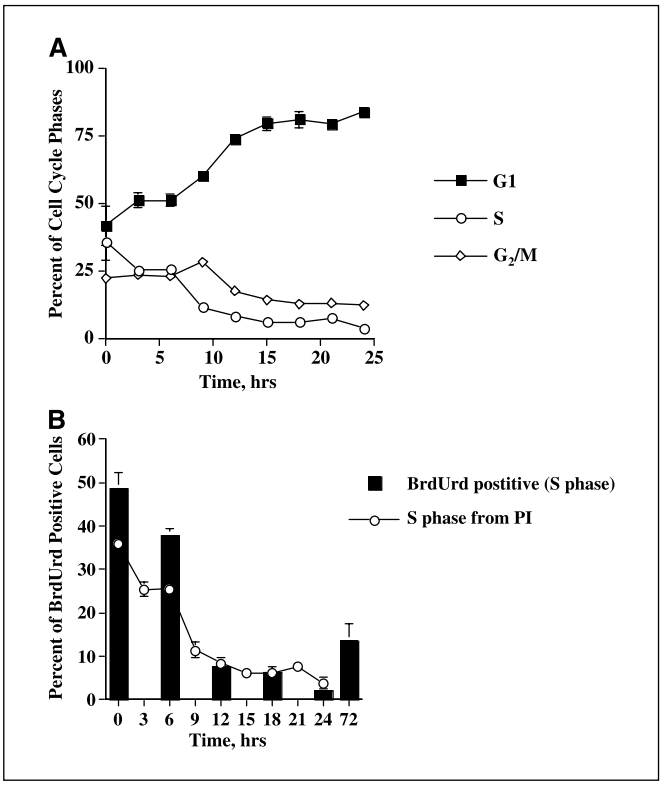

Figure 4. Staurosporine-mediated G_1 arrest occurs within 3 hours of treatment. *A,* the pRb^+ immortalized 76NE6 cells were treated with 4 nmol/L staurosporine. At the indicated times following treatment, sample cells were subjected to flow cytometry and the percent of each cell cycle phase was shown in the line graph with the G_1 (■), S (○), and G_2-M (◇) phases for each cell line. *B,* the 76NE6 pRb^+ cells were treated with staurosporine in the presence of BrdUrd. Cells were incubated with 1 μmol/L BrdUrd at 37°C for 20 minutes before harvest. *B,* percent S phase calculated from propidium staining (*line graph*) and from BrdUrd staining of cells treated with staurosporine (*bar graph*). The 72-hour time point represents cells treated with staurosporine for 24 hours, labeled with BrdUrd for 20 minutes, and then washed and allowed to recover for 48 hours.

cells were washed and incubated in drug-free medium for an additional 72 hours. Both BrdUrd incorporation (Fig. 4*B*) and flow cytometry analysis (data not shown) showed that removal of drug results in the resumption of DNA synthesis.

Next, to examine the role of staurosporine in modulating the progression of cells from G_1 to S phase, we used a "pulse-chase" strategy of BrdUrd incorporation (Fig. 5*A* and *B*). As schematically depicted in Fig. 5*A*, 76NE6 and 76NE7 cells were treated with BrdUrd for 20 minutes and then fresh medium in the presence or absence of 4 nmol/L staurosporine was added to the cells. At 3-hour intervals following BrdUrd treatment ±4 nmol/L staurosporine, cells were harvested and subjected to a two-color flow cytometric analysis with propidium iodine and BrdUrd. The results are presented as fraction of labeled divided cells (f_{ld}), representing the number of divided (or undivided) BrdUrd labeled cells as a fraction of the total number of cells stained with propidium iodide (Fig. 5*B*).

Figure 5*B* (*left*) depicts the fraction of labeled divided (f_{ld}) cells in the 76NE6 pRb^+ cells either treated with 4 nmol/L staurosporine (*closed symbols*) or untreated (*open symbols*). The results show that the untreated cells are progressing through the cell cycle without any perturbation as f_{ld} cells measure the fraction of cells entering each phase of the cell cycle, starting with cells in the S phase of the cell cycle (0 hours post BrdUrd labeling), progressing into G_2-M (3 hours post BrdUrd labeling), G_1 (12 hours post BrdUrd labeling), and the next S phase of the cell cycle (18 hours post BrdUrd labeling). Treatment with staurosporine perturbs the progression of cells past the G_1 phase of the cell cycle (Fig. 5*B, left, closed symbol*). Specifically, when cells reach the G_1 phase of the cell cycle (12 hours post BrdUrd labeling), there is no decrease in the amount of divided cells, indicating that cells have remained in the G_1 phase for the duration of the experiment. In the 76NE7 pRb^- cells (Fig. 5*B, right*), on the other hand, there is no perturbation of progression of cells through the different phases of the cell cycle in the presence or absence of staurosporine as measured by the fraction of BrdUrd-labeled and divided cells.

The third approach we took to examine the role of staurosporine in perturbing the progression of cells through different phases of the cell cycle was to first arrest the cells in G_2-M phase by a reversible mitotic blocker (i.e., nocodazole), release the cells from arrest, and then treat the cells with staurosporine (Fig. 5*C* and *D*). The question being addressed here is if pRb^+ cells, following arrest in G_2-M, can be subsequently arrested in the G_1 phase of the cell cycle by staurosporine. To address this question, we treated 76NE6 and 76NE7 cells with staurosporine alone (4 nmol/L), nocodazole alone, and nocodazole plus staurosporine. The scheme of the sequence of treatment with each condition is depicted in Fig. 5*C*. Following the different treatments, cells were subjected to flow cytometric analysis (Fig. 5*D*). The results revealed that whereas both cell lines were synchronized reversibly in the G_2-M phase of the cell cycle (*open circles*), only the 76NE6 cells were further arrested in the G_1 phase by staurosporine (*shaded diamonds*) and the 76NE7 cells continued through the cycle and were unperturbed by staurosporine. Specifically, in 76NE7 cells, the nocodazole alone and nocodazole plus staurosporine treatment arms resulted in identical progression out of G_1 phase (suggesting no arrest induced by staurosporine), whereas in 76NE6 cells, the nocodazole plus staurosporine–treated cells remained in the G_1 phase of the cell cycle and the nocodazole alone–treated cells progressed through G_1. Collectively, the results from Figs. 4 and 5 suggest that staurosporine can perturb the cell cycle of pRb^+ cells, but not of pRb^- cells.

pRb is directly modulated by staurosporine in mediating G_1 arrest. We next set out to directly examine the role of pRb in staurosporine-mediated G_1 arrest in the nonmalignant 76NE6 cells. To this end, mouse embryo fibroblasts from wild-type and $pRb^{-/-}$ mice (37, 38) were cultured and subjected to treatment with increasing concentrations of staurosporine (Fig. 6*A* and *B*). Flow cytometric analysis of treated cells indicated that whereas $pRb^{+/+}$ MEFs were very sensitive to staurosporine and accumulated in the G_1 phase of the cell cycle starting at 2 nmol/L (Fig. 6*A, top*), the $pRb^{-/-}$ MEFs were refractory to the cell cycle modulatory effects of staurosporine (Fig. 6*A, bottom*). The relative fold change of cells in G_1 phase in response to staurosporine treatment was 2.5-fold higher for $pRb^{+/+}$ MEFs as compared with $pRb^{-/-}$ MEFs (Fig. 6*B, left*). Western blot analysis revealed that CDK4 levels plummeted in response to staurosporine in $pRb^{+/+}$ cells, at concentrations as low as 1 nmol/L, whereas in $pRb^{-/-}$ MEFs, CDK4 basal levels were minimally decreased by staurosporine. CDK2 levels remained unaltered in both cells following staurosporine treatment (Fig. 6*B, right*).

The role of pRb was also assessed by down-regulation of pRb using siRNA in MDA-MB-231 cells that are wild-type for pRb (Fig. 6*C* and *D*). Down-regulation of pRb by siRNA resulted in a significant reduction in the amount of cells that accumulated in

the G_1 phase of the cell cycle (Fig. 6*C*). In these cells, the pRb protein was completely down-regulated by Rb siRNA sequences (Fig. 6*D*). The results from Fig. 6 suggest that staurosporine mediates G_1 arrest directly through the pRb pathway.

Discussion

Previous studies in our laboratory had investigated the use of staurosporine, a cytostatic drug, for protection of normal cells from the toxic effects of chemotherapy. From these studies, we determined that staurosporine, at low concentrations, maintains normal cells, but not tumor cells, in a reversible G_0-G_1 state. After treating the cells with staurosporine, the cells were subsequently treated with DNA-damaging agents (doxorubicin or camptothecin). The normal cells were protected due to the staurosporine-mediated G_1 arrest, without compromise of chemotoxicity against the tumor cells. The protection observed was in a p53-independent and pRb-dependent manner (2). Other labs have similarly revealed the importance of pRb in the staurosporine-mediated G_1 arrest process (3, 10–13).

In this article, we present a model for the staurosporine-mediated protection of nonmalignant cells with an intact Rb pathway. We find

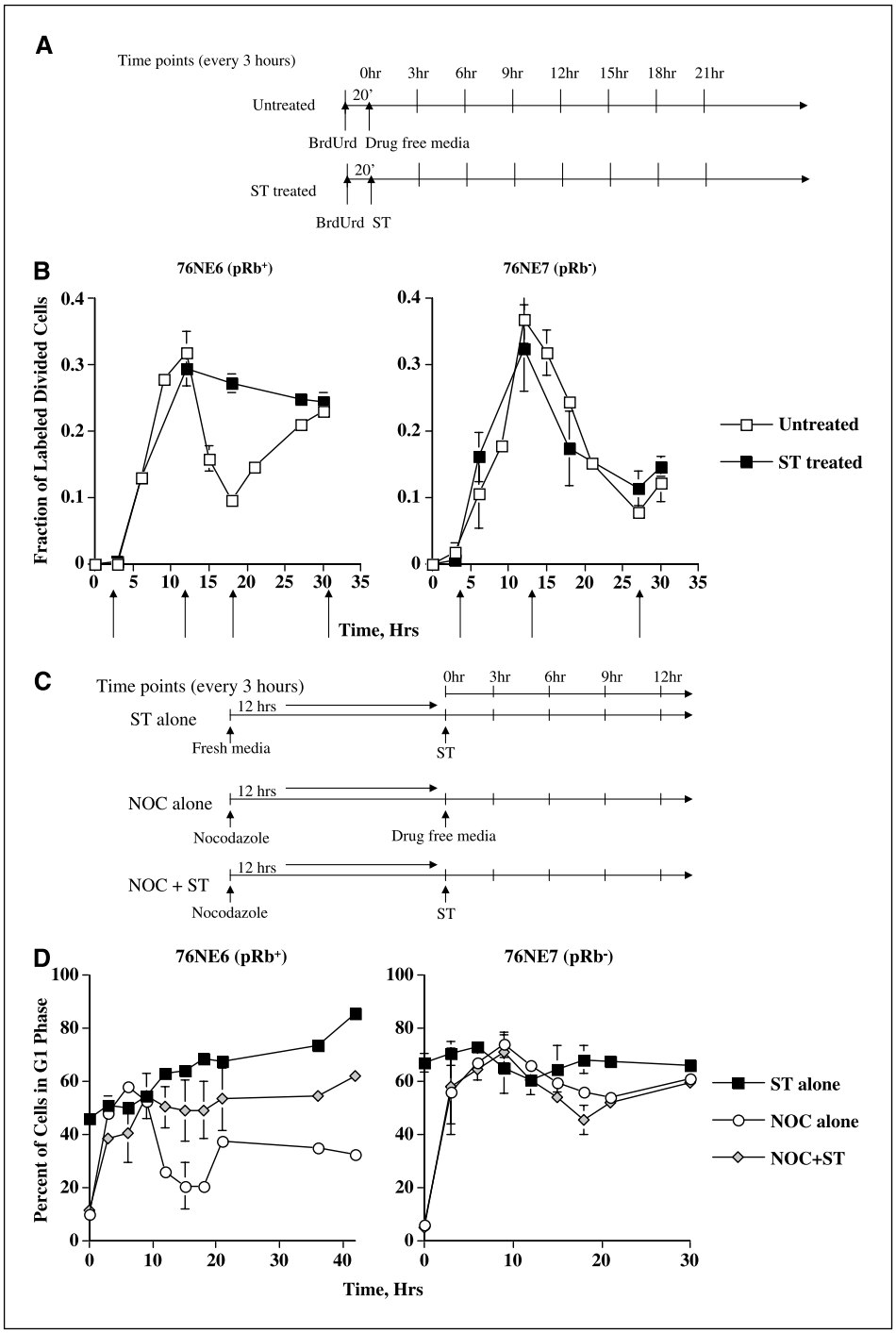

Figure 5. Cell cycle kinetics perturbed by staurosporine only in pRb^+ cells, but not in pRb^- cells. *A,* schematic of the time line for treatment. Cell lines were labeled with BrdUrd for 20 minutes (pulse), washed, and then either fresh medium or medium plus staurosporine was used as a chase. Fraction of labeled divided cells was calculated by taking the number of divided cells by the total amount of labeled cells. *B, left,* pRb^+ 76NE6 cells; *right,* pRb^- 76NE7 cells. *Arrows,* beginning of the different phases of the cell cycle (*first arrow,* G_2-M). *C,* schematic of the time line for nocodazole treatment. All cells were plated, allowed to adhere, and then washed with either fresh medium alone (*ST alone*) or fresh medium plus 0.125 μg/mL nocodazole (*NOC alone* and *NOC + ST*). Twelve hours posttreatment, all cells were washed with PBS and then fresh medium (*NOC alone*) or fresh medium plus 4 nmol/L staurosporine (*ST alone* and *NOC + ST*) was added to the cells. Time points were set every 3 hours after fresh medium or treatment with staurosporine, and the cells were processed for flow cytometric analysis with propidium iodide to determine the G_1 and G_2-M phases of the cell cycle. Shown is the G_1 phase for pRb^+ 76NE6 (*D, left*) and pRb^- 76NE7 (*D, right*) cells.

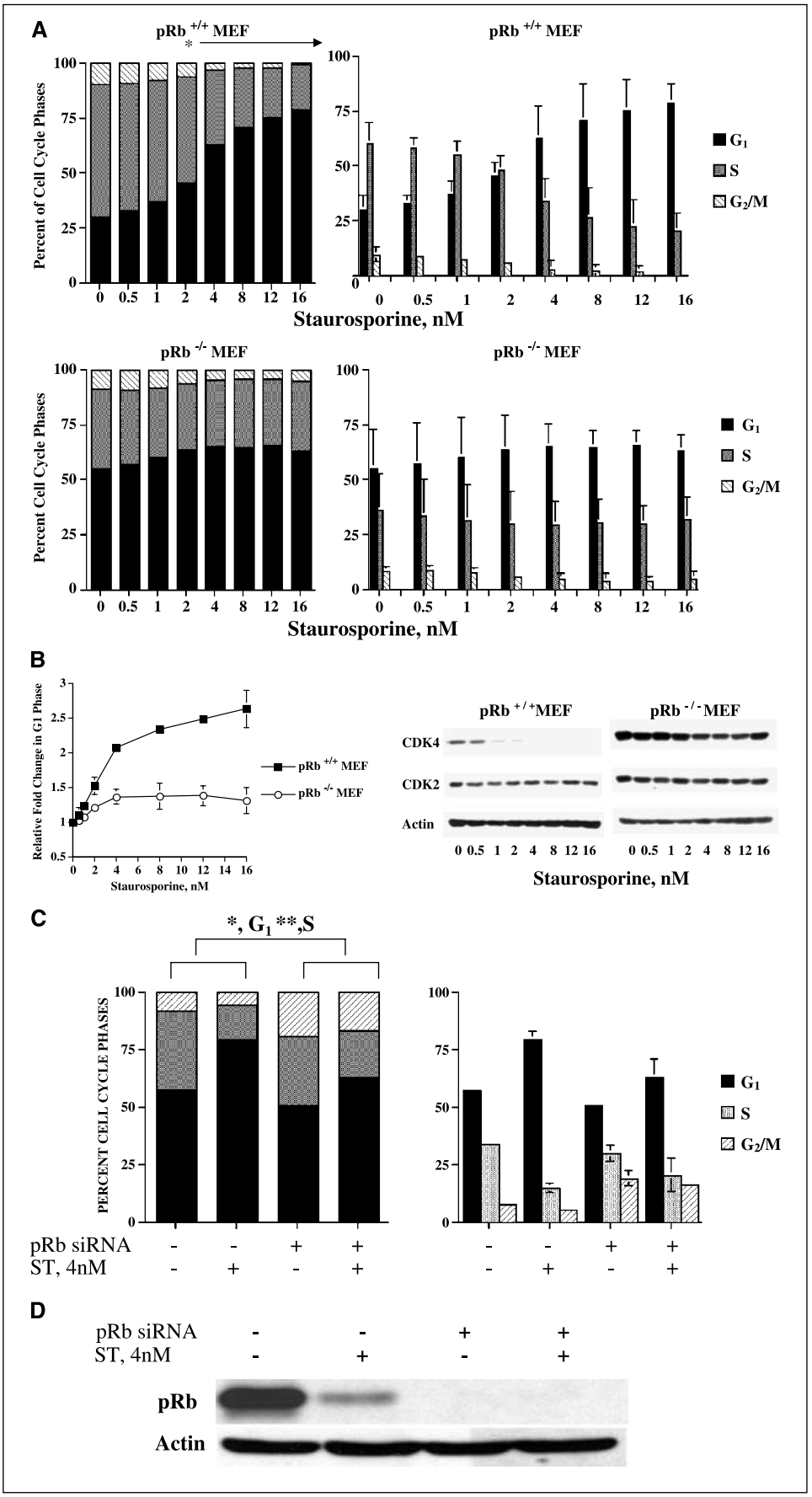

Figure 6. pRb protein is necessary for a G_1 arrest. *A, top,* $pRb^{+/+}$ MEFs; *bottom,* $pRb^{-/-}$ MEFs. MEFs were treated with seven concentrations of staurosporine (0.5-16 nmol/L). *Left,* cell cycle distribution was measured by flow cytometry and the percent of each cell cycle phase is shown in a bar graph form with the G_1 (*solid black columns*), S (*gray columns*), and G_2-M (*hatched columns*) phases for each of the cell lines. *Right,* data with error bars. Statistical calculations were done with GraphPad Prism 4 for Macintosh. The paired *t* test was done using a 95% confidence interval: *, $P = 0.05$; **, $P = 0.001$. *B, left,* relative fold change calculated from the full seven concentrations of staurosporine for the two cell lines. The relative fold change was calculated by dividing all of the staurosporine-treated cells in G_1 phase by the control cells (0 nmol/L staurosporine) in G_1 phase. *B, right,* $pRb^{+/+}$ MEF and $pRb^{-/-}$ MEF were treated with the indicated concentrations of staurosporine for 48 hours. Following treatment, cell lysates were prepared and subjected to Western blot analysis with the indicated antibodies and actin for equal loading. *C,* MDA-MB-231 cells (pRb^{+}) were transiently transfected for 24 hours with 30 nmol/L of predesigned siRNA to the *Rb1* gene (Ambion). Cells treated with 4 nmol/L staurosporine were treated 72 hours after transfection for an additional 24 hours, and all cells (treated and control) were harvested 96 hours after initial transfection. Samples were subjected to flow cytometry and the percent of each cell cycle phase is shown in a bar graph form with the G_1 (*solid black columns*), S (*gray columns*), and G_2-M (*hatched columns*) phases for each of the cell lines. *Right,* data with error bars. Statistical calculations were done with GraphPad Prism 4 for Macintosh. The paired *t* test was done with a 95% confidence interval: *, $P = 0.05$; **, $P = 0.001$. *D,* cell lysates from the same samples were prepared and subjected to Western blot analysis with the indicated antibodies, with actin for equal loading.

that staurosporine acts directly on the pRb pathway and results in the decrease of CDK4 expression. The resultant decrease in CDK4 protein levels leads to inactivation of CDK4, which is no longer able to phosphorylate pRb. With CDK4 no longer active, pRb remains hypophosphorylated, leading to the G_1 arrest.

The scenario described above is applicable to our immortalized cell model of 76NE6 ($pRb^+/p53^-$) cells, in which case p21 regulation is p53 independent. However, in the case of our normal mortal cells, which are $p53^+$, p21 is p53 dependent and follows the same expression pattern as p53. In the normal cells ($p53^+/pRb^+$), CDK4 plays a greater role in the staurosporine-mediated G_1 arrest because in these cells, we do not see an increase in p21, only an increase in p27 at the higher concentrations of staurosporine. Furthermore, the pRb^+ 76NE6 cells have a lower concentration of CDK4 protein than the pRb^- 76NE7 cells. In the pRb^+ 76NE6 cells, any slight change in CDK4 expression level has a marked effect on the cell cycle, in this case leading to a G_1 arrest. Staurosporine may have no effect on cells with overexpression of CDK4 regardless of pRb status. Staurosporine may be able to reduce the amount of CDK4 in these cells, but such reduction is not sufficient to mediate a G_1 arrest. Additionally, the remaining amount of CDK4 in these pRb^- cells may be enough to keep p21 bound and allow CDK4 to remain active. Therefore, in tumors that still have an intact pRb protein, but overexpressing CDK4, staurosporine will not protect these cells but will still protect the normal cells.

The idea for a protection strategy was described in the 1970s by several labs (39–41). However, since then, most labs have focused on the ability to increase the toxicity to tumor cells with existing agents by abrogating the S or G_2-M phase of the cell cycle. An example of this is the staurosporine analogue 7-hydroxystaurosporine (UCN-01). When used after the addition of cytotoxic agents (i.e., camptothecin or fludarabine nucleoside), UCN-01 has proved to enhance the cytotoxicity of these agents (42–46).

Our strategy is different, however, because we are treating the cells with staurosporine beforehand to protect the normal cells from the cytotoxic agent, instead of enhancing the effect of the cytotoxic agent on the tumor cells. Both strategies are taking advantage of the cell cycle and are important for understanding the drugs we use for chemotherapy.

In an *in vitro* setting, staurosporine has proved to be a very promising agent in the strategy to protect normal cells from the toxic effects of chemotherapeutic agents. However, in trials with UCN-01, it has been shown to bind to the α1 acid glycoprotein in human plasma, causing a prolonged half-life of the drug and low clearance (47, 48). This could be a limitation with staurosporine *in vivo* and has been shown to be a hindrance in several studies with UCN-01 (49–52). The clinical limitations noted with UCN-01 highlight the need for additional understanding of drug metabolism, half-life, and reversibility before implementation of a protection strategy in cancer patients.

Acknowledgments

Received 5/17/2006; revised 6/26/2006; accepted 7/25/2006.

Grant support: NIH grant R01-CA87458 (K. Keyomarsi) and NIH Cancer Center grant P30-CA16672.

The costs of publication of this article were defrayed in part by the payment of page charges. This article must therefore be hereby marked *advertisement* in accordance with 18 U.S.C. Section 1734 solely to indicate this fact.

We thank the M.D. Anderson Cancer Center for the use of their tissue culture, flow cytometry, and DNA sequencing core facilities, Dr. Rafael Herrera at the Baylor College of Medicine for the $pRb^{+/+}$ and $pRb^{-/-}$ MEF cell lines, and Nalini Patel for her help with the BrdUrd work.

References

1. Keyomarsi K, Pardee AB. Selective protection of normal proliferating cells against the toxic effects of chemotherapeutic agents. Prog Cell Cycle Res 2003;5:527–32.
2. Chen X, Lowe M, Herliczek T, et al. Protection of normal proliferating cells against chemotherapy by staurosporine-mediated, selective, and reversible G(1) arrest. J Natl Cancer Inst 2000;92:1999–2008.
3. Stone S, Dayananth P, Kamb A. Reversible, p16-mediated cell cycle arrest as protection from chemotherapy. Cancer Res 1996;56:3199–202.
4. Ashizawa S, Nishizawa H, Yamada M, et al. Collective inhibition of pRB family proteins by phosphorylation in cells with p16INK4a loss or cyclin E overexpression. J Biol Chem 2001;276:11362–70.
5. Ortega S, Malumbres M, Barbacid M. Cyclin D-dependent kinases, INK4 inhibitors and cancer. Biochim Biophys Acta 2002;1602:73–87. Review.
6. Malumbres M, Barbacid M. To cycle or not to cycle: a critical decision in cancer. Nat Rev Cancer 2001;1:222–31.
7. Shimizu E, Zhao MR, Nakanishi H, et al. Differing effects of staurosporine and UCN-01 on RB protein phosphorylation and expression of lung cancer cell lines. Oncology 1996;53:494–504.
8. Weinberg RA. The retinoblastoma protein and cell cycle control. Cell 1995;81:323–30.
9. Classon M, Harlow E. The retinoblastoma tumour suppressor in development and cancer. Nat Rev Cancer 2002;2:910–7.
10. Schnier JB, Gadbois DM, Nishi K, Bradbury EM. The kinase inhibitor staurosporine induces G_1 arrest at two points: effect on retinoblastoma protein phosphorylation and cyclin-dependent kinase 2 in normal and transformed cells. Cancer Res 1994;54:5959–63.
11. Schnier JB, Nishi K, Goodrich DW, Bradbury EM. G_1 arrest and down-regulation of cyclin E/cyclin-dependent kinase 2 by the protein kinase inhibitor staurosporine are dependent on the retinoblastoma protein in the bladder carcinoma cell line 5637. Proc Natl Acad Sci U S A 1996;93:5941–6.
12. Orr MS, Reinhold W, Yu L, Schreiber-Agus N, O'Connor PM. An important role for the retinoblastoma protein in staurosporine-induced G_1 arrest in murine embryonic fibroblasts. J Biol Chem 1998;273:3803–7.
13. Zhou W, Lin Y, Wersto R, Chrest J, Gabrielson E. Staurosporine-induced G(1) arrest in cancer cells depends on an intact pRB but is independent of p16 status. Cancer Lett 2002;183:103–7.
14. Gescher A. Staurosporine analogues—pharmacological toys or useful antitumour agents? Crit Rev Oncol Hematol 2000;34:127–35.
15. Pickett CA, Manning N, Akita Y, Gutierrez-Hartmann A. Role of specific protein kinase C isozymes in mediating epidermal growth factor, thyrotropin-releasing hormone, and phorbol ester regulation of the rat prolactin promoter in GH4/GH4C1 pituitary cells. Mol Endocrinol 2002;16:2840–52.
16. Meijer L. Chemical inhibitors of cyclin-dependent kinases. Prog Cell Cycle Res 1995;1:351–63.
17. Konstantinidis AK, Radhakrishnan R, Gu F, Rao RN, Yeh WK. Purification, characterization, and kinetic mechanism of cyclin D1. CDK4, a major target for cell cycle regulation. J Biol Chem 1998;273:26506–15.
18. Gadbois DM, Peterson S, Bradbury EM, Lehnert BE. CDK4/cyclin D1/PCNA complexes during staurosporine-induced G_1 arrest and G_0 arrest of human fibroblasts. Exp Cell Res 1995;220:220–5.
19. Zong Z-P, Fujikawa-Yamamoto K, Li A-L, et al. Both low and high concentrations of staurosporine induce G_1 arrest through down-regulation of cyclin E and cdk2 expression. Cell Struct Funct 1999;24:457–63.
20. Shimizu TTN, Tachibana K, Takeda K. Complex regulation of CDK2 and G_1 arrest during neuronal differentiation of human prostatic cancer TSU-Prl cells by staurosporine. Anticancer Res 2001;21:893–8.
21. Kwon TK, Buchholz MA, Chrest FJ, Nordin AA. Staurosporine-induced G_1 arrest is associated with the induction and accumulation of cyclin-dependent kinase inhibitors. Cell Growth Differ 1996;7:1305–13.
22. Zeng YX. el-Deiry WS. Regulation of p21WAF1/CIP1 expression by p53-independent pathways. Oncogene 1996;12:1557–64.
23. Liu Y, Chen JJ, Gao Q, et al. Multiple functions of human papillomavirus type 16 E6 contribute to the immortalization of mammary epithelial cells. J Virol 1999;73:7297–307.
24. Gao Q, Srinivasan S, Boyer SN, Wazer DE, Band V. The E6 oncoproteins of high-risk papillomaviruses bind to a novel putative GAP protein, E6TP1, and target it for degradation. Mol Cell Biol 1999;19:733–44.
25. Dalal S, Gao Q, Androphy EJ, Band V. Mutational analysis of human papillomavirus type 16 E6 demonstrates that p53 degradation is necessary for immortalization of mammary epithelial cells. J Virol 1996;70:683–8.
26. Chen JJ, Reid CE, Band V, Androphy EJ. Interaction of papillomavirus E6 oncoproteins with a putative calcium-binding protein. Science 1995;269:529–31.
27. Band V. Preneoplastic transformation of human mammary epithelial cells. Semin Cancer Biol 1995;6:185–92.
28. Wazer DE, Liu XL, Chu Q, Gao Q, Band V. Immortalization of distinct human mammary epithelial cell types by human papilloma virus 16 E6 or E7. Proc Natl Acad Sci U S A 1995;92:3687–91.
29. Band V, Dalal S, Delmolino L, Androphy EJ. Enhanced degradation of p53 protein in HPV-6 and BPV-1 E6-immortalized human mammary epithelial cells. EMBO J 1993;12:1847–52.
30. Band V, De Caprio JA, Delmolino L, Kulesa V, Sager R.

Loss of p53 protein in human papillomavirus type 16 E6-immortalized human mammary epithelial cells. J Virol 1991;65:6671–6.
31. Band V, Zajchowski D, Kulesa V, Sager R. Human papilloma virus DNAs immortalize normal human mammary epithelial cells and reduce their growth factor requirements. Proc Natl Acad Sci U S A 1990;87:463–7.
32. Ratsch SB, Gao Q, Srinivasan S, Wazer DE, Band V. Multiple genetic changes are required for efficient immortalization of different subtypes of normal mammary epithelial cells. Radiat Res 2001;155:143–50.
33. Keyomarsi K, Pardee A. Redundant cyclin overexpression and gene amplification in breast cancer cells. Proc Natl Acad Sci U S A 1993;90:1112–6.
34. Keyomarsi K, Conte D, Jr., Toyofuku W, Fox MP. Deregulation of cyclin E in breast cancer. Oncogene 1995;11:941–50.
35. Terry NH, White RA. Cell cycle kinetics estimated by analysis of bromodeoxyuridine incorporation. Methods Cell Biol 2001;63:355–74.
36. Rao S, Lowe M, Herliczek TW, Keyomarsi K. Lovastatin mediated G_1 arrest in normal and tumor breast cells is through inhibition of CDK2 activity and redistribution of p21 and p27, independent of p53. Oncogene 1998;17:2393–402.
37. Lipinski MM, Jacks T. The retinoblastoma gene family in differentiation and development. Oncogene 1999;18:7873–82.
38. Lin BT, Gruenwald S, Morla AO, Lee W-H, Wang JYL. Retinoblastoma cancer suppressor gene product is a substrate of the cell cycle regulator cdc2 kinase. EMBO J 1991;10:857–64.
39. Lieberman MW, Verbin RS, Landay M, et al. A probable role for protein synthesis in intestinal epithelial cell damage induced *in vivo* by cytosine arabinoside, nitrogen mustard, or X-irradiation. Cancer Res 1970;30:942–51.
40. Bhuyan BK, Fraser TJ. Antagonism between DNA synthesis inhibitors and protein synthesis inhibitors in mammalian cell cultures. Cancer Res 1974;34:778–82.
41. Pardee AB, James LJ. Selective killing of transformed baby hamster kidney (BHK) cells. Proc Natl Acad Sci U S A 1975;72:4994–8.
42. Shao RG, Cao CX, Shimizu T, O'Connor PM, Kohn KW, Pommier Y. Abrogation of an S-phase checkpoint and potentiation of camptothecin cytotoxicity by 7-hydroxystaurosporine (UCN-01) in human cancer cell lines, possibly influenced by p53 function. Cancer Res 1997;57:4029–35.
43. Akinaga S, Nomura K, Gomi K, Okabe M. Enhancement of antitumor activity of mitomycin C *in vitro* and *in vivo* by UCN-01, a selective inhibitor of protein kinase C. Cancer Chemother Pharmacol 1993;32:183–9.
44. Wang Q, Fan S, Eastman A, Worland PJ, Sausville EA, O'Connor PM. UCN-01: a potent abrogator of G_2 checkpoint function in cancer cells with disrupted p53. J Natl Cancer Inst 1996;88:956–65.
45. Sugiyama K, Shimizu M, Akiyama T, et al. UCN-01 selectively enhances mitomycin C cytotoxicity in p53 defective cells which is mediated through S and/or G(2) checkpoint abrogation. Int J Cancer 2000;85:703–9.
46. Sampath D, Shi Z, Plunkett W. Inhibition of cyclin-dependent kinase 2 by the Chk1-25A pathway during the S-phase checkpoint activated by fludarabine: dysregulation by 7-hydroxystaurosporine. Mol Pharmacol 2002;62:680–8.
47. Fuse E, Tanii TH, Takai K, et al. Altered pharmacokinetics of a novel anticancer drug, UCN-01, caused by specific high affinity binding to α1-acid glycoprotein in humans. Cancer Res 1999;59:1054–60.
48. Swannie HC, Kaye SB. Protein kinase C inhibitors. Curr Oncol Rep 2002;4:37–46.
49. Hedaya MA, Daoud SS. Tissue distribution and plasma pharmacokinetics of UCN-01 at steady-state and following bolus administration in rats: influence of human α1-acid glycoprotein binding. Anticancer Res 2001;21:4005–10.
50. Fuse E, Hashimoto A, Sato N, et al. Physiological modeling of altered pharmacokinetics of a novel anticancer drug, UCN-01 (7-hydroxystaurosporine), caused by slow dissociation of UCN-01 from human α1-acid glycoprotein. Pharm Res 2000;17:553–64.
51. Fuse E, Tanii H, Kurata N, et al. Unpredicted clinical pharmacology of UCN-01 caused by specific binding to human α1-acid glycoprotein. Cancer Res 1998;58:3248–53.
52. Fuse E, Tanii H, Takai K, et al. Altered pharmacokinetics of a novel anticancer drug, UCN-01, caused by specific high affinity binding to α1-acid glycoprotein in humans. Cancer Res 1999;59:1054–60.

The Differential Staurosporine-Mediated G_1 Arrest in Normal versus Tumor Cells Is Dependent on the Retinoblastoma Protein

Mollianne McGahren-Murray, Nicholas H.A. Terry and Khandan Keyomarsi

Cancer Res 2006;66:9744-9753.